

Article

New Constraints on the Main Mineralization Event Inferred from the Latest Discoveries in the Bor Metallogenetic Zone (BMZ, East Serbia)

Miodrag Banješević ^{1,*}, Vladica Cvetković ², Albrecht von Quadt ³ ,
Darivojka Ljubović Obradović ⁴, Nebojša Vasić ², Aleksandar Pačevski ² and Irena Peytcheva ⁵

¹ Technical Faculty in Bor, University of Belgrade, Vojske Jugoslavije 12, 19210 Bor, Serbia

² Faculty of Mining and Geology, University of Belgrade, Dušina 7, 11000 Belgrade, Serbia; vladica.cvetkovic@rgf.bg.ac.rs (V.C.); sedimentologija@yahoo.com (N.V.); aleksandar.pacevski@rgf.bg.ac.rs (A.P.)

³ Institute of Geochemistry and Petrology, Eth Zurich, Clausiusstrasse 25, 8092 Zurich, Switzerland; albrecht.vonquadt@erdw.ethz.ch

⁴ Geological Survey of Serbia, Rovinjska 12, 11000 Belgrade, Serbia; office@gzs.gov.rs

⁵ Geological Institute, Bulgarian Academy of Science, Acad. G. Bonchev Str., Bl. 24, 1113 Sofia, Bulgaria; peytcheva@erdw.ethz.ch

* Correspondence: mbanjesevic@tfbor.bg.ac.rs

Received: 31 August 2019; Accepted: 21 October 2019; Published: 31 October 2019



Abstract: This study aims at better constraining the link between magmatism and metallogeny in the south-easternmost sector of the Bor Metallogenetic Zone (BMZ), where the world-class copper and gold deposit of Čukaru Peki was recently discovered. The obtained U/Pb zircon ages confirm the earlier knowledge that the major Cu–Au porphyry and epithermal mineralization in the BMZ is genetically related to the first volcanic phase (‘Timok andesite’; 85–90 Ma). However, the data also suggest that during this phase, two subgroups of andesite porphyry were formed; they are named volcanic phase 1A (V1A) and volcanic phase 1B (V1B). The V1A andesite (89–90 Ma) is plagioclase-hornblende phyric, holocrystalline and ubiquitously hydrothermally altered and/or mineralized, whereas the V1B (85–86 Ma) is hornblende-plagioclase phyric, holo- to hypocrySTALLINE, fresh, and non-mineralized. According to our simplified model, the contrasting productivity of the V1A and V1B is explained by fluctuations during AFC (assimilation-fractional crystallization) processes of water-rich parental magma, which have controlled the order of crystallization of hornblende and plagioclase in the V1A and V1B andesite.

Keywords: andesite; Balkan Peninsula; hydrothermal events; porphyry copper deposits; Tethyan Metallogenetic Belt

1. Introduction

The Bor Metallogenetic Zone (BMZ) is part of the Late Cretaceous Apuseni-Banat-Timok-Srednogorje Belt (ABTS; [1,2]), which belongs to the transcontinental Tethyan-Eurasian Metallogenic Belt [3]. Originally, the ABTS was a continuous west/north–west–east/south–east striking belt; however, in present day geotectonic configuration, it is geographically separated into three different sectors. The easternmost sector is Srednogorje and it has preserved the original W–E orientation of the entire belt. The latter two sectors: Timok and Banat-Apuseni are currently elongated N–S, due to Cenozoic (Miocene) clockwise rotations that produced a sharp inflection between the Timok and Srednogorje parts [4–6].

The ABTS is known to host some of the largest copper and gold deposits in Europe and its geology has been frequently studied in the last several decades (e.g., [2,7–13], among others). The studies have covered various geological aspects of the origin and evolution of this belt and established a solid genetic link between magmatic and mineralization processes. This knowledge is mainly based on stratigraphic relationships and geochronological data, including Ar–Ar [8,9], U–Pb zircon (e.g., [2,11,13]) and Re–Os molybdenite dating [10].

The geochronological data indicate that the ABTS belt exhibits a regular distribution of radiometric ages of mineralization and magmatism and that these patterns are discernible both along and across strike. Thus, [9,10] suggest that mineralization shows a decrease in age along strike, from the Srednogorje (87–92 Ma), throughout the Timok- (81–88 Ma) up to the Banat–Apuseni sector (72–83 Ma) [14]; in addition, the respective mineralization events were mostly short-lived, i.e., <1 m.y. Such an along-strike pattern is less obvious concerning the age of the accompanying igneous rocks; namely, each sector encompasses similar age ranges with almost 90% of radiometric data falling between 70 Ma and 90 Ma [12]. On the other hand, the Timok and the Srednogorje sectors display a well-developed across-strike age shift in which magmatic rocks become progressively younger towards the west and south, respectively. Although these age patterns were discussed by many authors (e.g., [11,12,15]), there is still a number of issues that are not fully understood, for instance: (a) What is the immediate cause of the observed regularity in age distribution along and across strike? (b) What is the tectonothermal relationship between these two types of age patterns? (c) Why are the patterns less observable or even absent in some areas? In order to tackle any of these important regional questions it is necessary to increase our present-day knowledge at a more local scale, particularly regarding the link between magmatism and mineralization.

In this study, we address the geology of the south-eastern part of the Bor Metallogenic Zone. The BMZ represents the entire Timok sector of the ABTS belt and is usually referred to as the Timok Magmatic Complex (TMC). The BMZ is famous for its large porphyry copper systems accompanied by epithermal high-sulphidation Cu–Au ore deposits and subordinate low-sulphidation Cu–Au mineralization. More than 25 individual or cluster-like Cu–Au orebodies occurred in the BMZ, mostly as veins, breccia matrix or total replacement by massive sulphides; the massive ore is mainly composed by enargite, covellite and chalcocite with ubiquitous pyrite, and with average grades of 2% Cu and 1.3 g/t Au [16–19].

Previous studies in the BMZ (e.g., [2,8–11,13]) in combination with those from adjacent areas in the ABTS region (e.g. [7,12] etc.) have provided important knowledge that can be summarized as follows: (a) magmatism in the BMZ commenced by the beginning of the Turonian (≥ 90 Ma); (b) magmatic events started to develop in the easternmost area of the BMZ, and became progressively younger towards the west; (c) the first volcanic phase (eastern area) hosted the most economically significant copper and gold deposits in the BMZ; and (d) the second volcanic phase (western area) was much less productive in terms of mineralization.

The recent discovery of a world class copper and gold deposit in the area of Čukaru Peki seriously aroused new interests for further investigating the BMZ, both in the exploration and the scientific context. Some of the new data obtained on the recovered drill-cores were recently published by Zijin Mining Group Co. Ltd., Reservoir Minerals Inc. and others [20–22].

The major goal of our study was to refine the link between the first volcanic phase and the major mineralization process responsible for the formation of the largest epithermal-porphyry systems in the BMZ. We present data on stratigraphic and geological relationships (field observations) and exploration drilling at nearby Nikoličevo as well as a set of new U/Pb zircon ages on volcanic rocks from the recovered drill holes.

The results of our study confirm that the major mineralization in the BMZ formed during the first volcanic phase but they also show that the first volcanic phase comprises both mineralized and non-mineralized volcanic rocks. The observed petrographic variations shown by almost

contemporaneous volcanic rocks characterized by different ore productivity can be effectively used as prospection criteria when investigating similar ore deposits worldwide [23–25].

2. Geology of the BMZ

The overlapping areas of the BMZ and the TMC represent a significant part of the East-Serbian Carpatho-Balkanides (see inset of Figure 1), which belong to the larger Alpine-Carpathian-Dinaride orogen (e.g., [26]). Recent studies [11–13] argue in favour of an already existing hypothesis (e.g., [2]) that the volcano-plutonic provinces of the entire ABTS belt formed in response to Late Cretaceous subduction processes along the Eurasian active margin.

The geology of the TMC, the location of the main ore deposits of the BMZ, the available age determinations, as well as the locations of the Čukaru Peki and the Nikoličevo area (rectangles) are given in Figure 1. The TMC predominantly consists of extrusive volcanics and volcanoclastics that are associated with volcano-sedimentary and sedimentary rock series. The entire TMC generally formed from Turonian to Campanian/Paleogene times as indicated by the available radiometric ages (predominantly K-Ar) covering a span from 90 Ma to 62 Ma ([27–31], etc.). Several recent studies that combined high-precision geochronology and stratigraphic and petrological information [7,8,10,11,14,32,33] reveal that there is a steady westward decrease in the age of magmatic products, accompanied by slight to moderate changes in rock composition (e.g., [11,30]).

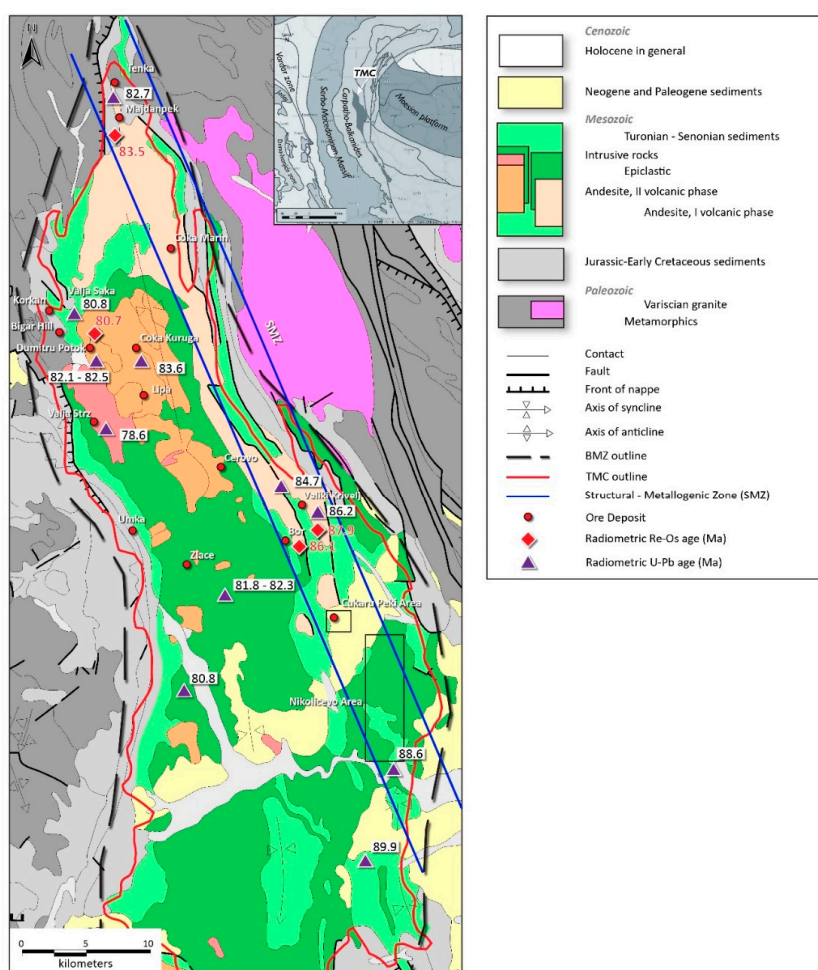


Figure 1. A geological-metallogenetic map of the Timok Magmatic Complex (TMK) and the Bor Metallogenetic Zone (BMZ); the numbers are literature U-Pb and Re-Os age data [7,10,11,13,32]; the inset shows the regional geotectonic position; note that the legend is organized in the form of a simplified geological column.

The TMC evolution is roughly separated into three volcanic phases, which have been known for more than half a century (e.g., [34]). It is worth noting that true intrusions are scarcely exposed in this area, therefore, the age and evolution of the entire TMC have been interpreted by investigating volcanic rocks including small-size dykes and/or irregularly-shaped subvolcanic bodies. Hence, in the easternmost part of the TMC, predominate volcanic rocks of biotite-hornblende andesite (\pm dacite) compositions known in the Serbian literature as ‘Timok andesites’ (Andesite, first volcanic phase in Figure 1). They are mostly represented by subaerial to shallow-water extrusive volcanic and volcanoclastic rocks accompanied by rare shallow intrusive bodies. These rocks stratigraphically overlie the Cenomanian siliclastic sediments (not shown in Figure 1) and are partly covered by volcano-sedimentary rocks (Epiclastic in Figure 1). The available U/Pb zircon ages of the 1st phase volcanic rocks range from 89–84 Ma [11,15,32,33]. Turonian-Senonian clastic sediments are continuously developed and can be found over the volcanic basement but also as underlying or overlying the products of the first volcanic phase.

In the west, the volcanic rocks of the first phase transition into the second phase hornblende-pyroxene- to pyroxene andesite and basaltic andesite; the latter are predominantly emplaced as submarine extrusive volcanics and associated epiclastic rocks (Andesite, second volcanic phase in Figure 1). These volcanic rocks reveal a U/Pb zircon age range of 83–80 Ma [11,15,32,33]. They are also stratigraphically interlayered with the above-mentioned Turonian-Senonian sediments and are commonly covered by epiclastic products (Epiclastic in Figure 1; note that epiclastic deposits are shown as a single unit).

In the westernmost part of the TMC occur rare plutonic and shallow intrusive rocks of monzodiorite–granodiorite–gabbrodiorite compositions (Intrusive rocks in Figure 1). The largest mass is called Valja Strž, which is dated at 82.5–78.6 Ma [13,32]. Further to the west, numerous small-volume dykes and irregularly shaped shallow intrusions of latitic and trachyandesitic compositions occur (not shown in Figure 1). These subvolcanic rocks cut the above-mentioned volcanic rocks of the second phase, therefore, the earlier authors considered them products of the so-called third volcanic phase (e.g., [34]).

The BMZ hosts more than 100 significant metallic occurrences out of which 22 have been considered ore deposits (see review of [18]). The locations of the 14 most economically significant ore deposits are indicated in Figure 1. Four copper deposits are presently in operation: Majdanpek, Veliki Krivelj, Bor, and Cerovo.

The world-class epithermal high-sulphidation Cu–Au deposit of Bor and large porphyry Cu–Au deposits of Veliki Krivelj, Majdanpek and Bor-Borska Reka are all located along the eastern margin of the BMZ, more precisely inside a narrow structural-metallogenetic zone-oriented NNW-SSE (blue lines in Figure 1). The Veliki Krivelj, Majdanpek and Bor-Borska Reka deposits are porphyry systems, although without a directly observable relationship to underlying plutons. In the same structural-metallogenetic zone occur smaller epithermal deposits of high-sulphidation, such as Čoka Marin [35,36], which do not exhibit obvious links to larger porphyry systems.

The structural-metallogenetic zone along the eastern margin of the BMZ is probably one of the most prospective areas in Europe in terms of exploration. This view is corroborated by the recent discovery of very rich epithermal and porphyry copper and gold mineralization of Čukaru Peki, which was found exactly along the southern continuation of the same zone.

By contrast, the western part of the BMZ is less promising and hosts generally different morphogenetic types of mineralization [13,19]. There are smaller porphyry Cu–Au, high sulphidation-style, polymetallic replacement, and skarn-type deposits connected with plutonic rocks (e.g., Tenka, Valja Saka, Umka, Dumitru Potok, Čoka Kuruga, Valja Strž, Lipa, among others). This zone also hosts the low-sulphidation deposit of Zlaće and the sediment-hosted Au mineralization Korkan-Bigar Hill [13,37]. In the last several years, occurrences of manganese ore were also reported in this part of the TMC, and they are interpreted as VMS/SEDEX-type of mineralization [13,19,38].

3. Sampling and Methods

We studied five drill-cores from which a total of 51 rock samples were investigated by optical microscopy, 20 samples were characterized paleontologically, whereas sedimentological analyses were carried out on 53 samples. Seven samples of volcanic rocks were analysed radiometrically by U/Pb zircon age determinations. The zircons were sieved into specific fractions (<63 μm , 63–250 μm , >250 μm), concentrated using magnetic, heavy liquid separation (Methylene Iodide) and finally hand-picked, embedded in epoxy resin, and polished. Prior to U/Pb analyses, the zircons were characterized by cathodoluminescence and back-scattered electron detectors (JEOL 1066 LV) in order to identify potential inherited cores, inclusions and other crystal inclusions.

Spots of 30 μm in diameter within the zircons were selected based on the obtained CL images. Generally, one spot was chosen in the interior (core) and one in the exterior (rim) part of the zircon with further spots selected after individual evaluation of the CL image. In-situ U-Pb geochronology were conducted by laser ablation inductively-coupled plasma mass spectrometry (LA-ICP-MS) at the Institute of Geochemistry and Petrology, ETH Zurich using a 193-nm Resolution (S155) ArF excimer laser coupled to an Element SF ICP-MS. The output energy was typically ca. 2 J/cm² and a 5 Hz pulse repetition rate was used. The ablation was under helium flow of 0.7 L/min. Argon was admixed to the aerosol within the funnel of the ablation cell to transport the ablated material to the ICP for ionization. Dwell times range from 5–30 ms and peak hopping was applied. Oxide generation was optimized at ThO⁺/Th⁺ = <0.3%. For each analysis, a baseline was measured for 25 s followed by 40 s of ablation. Elemental concentrations were calculated using the IGOR-based Iolite software [39].

For U-Pb geochronology, the masses 202, 204, 206, 207, 208, 232, 235 and 238 were measured. Total ablation time was set to 30 s with a gas blank/background measurement of 10 s. Age data were collected in runs of 20 samples bracketed before and after by two analyses of the primary reference material GJ-1 [40] and each one of secondary reference zircons 91500 [41], Temora [42], Plesovice [43] and AusZ7.7 [44]. Data reduction was performed with the IGOR-based Iolite V3.6 [39] and Vizual Age [45] software. Obtained isotope ratios and dates are corrected for mass bias, instrumental drift and downhole fractionation using primary reference material. Analysed ages and trace elements of spots with elevated Al, P, Ca, Mn or Fe were discarded as these values indicate the presence of mineral (e.g., apatite, feldspar) or melt inclusions. Age calculation and plots have been performed with the IsoplotR tool [46].

4. Results

4.1. Geology and Petrography

Geology of the areas of Nikoličevo and Čukaru Peki as well as the exact locations of the drill holes are given in a geological map (Figure 2) and in stratigraphic logs (Figures 3 and 4).

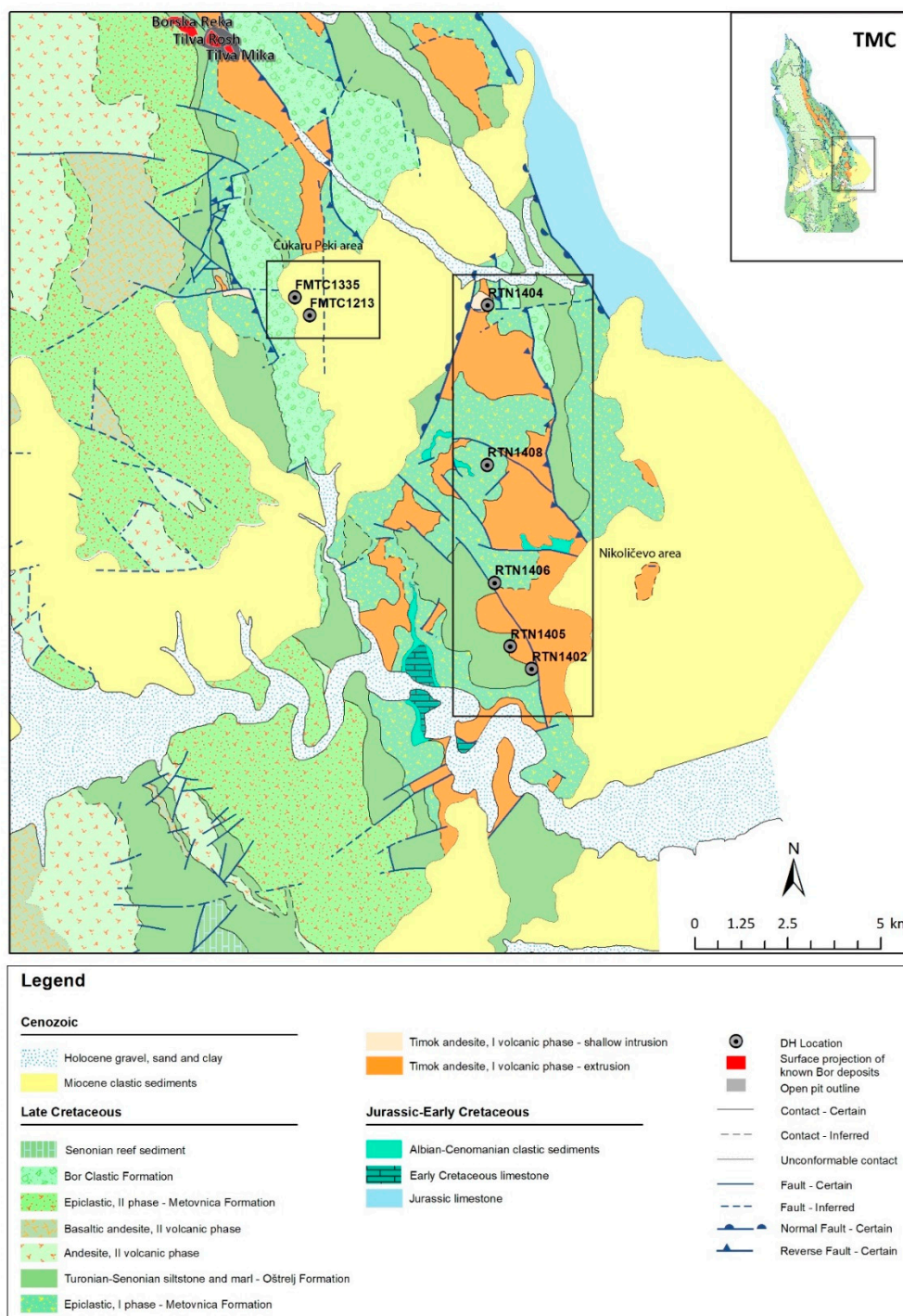


Figure 2. A detailed geological map of the areas of Čukaru Peki and Nikoličevo.

All the studied drill-cores exhibit a similar lithology consisting of a complex series of Late Cretaceous volcanic, volcano-sedimentary and sedimentary rocks. The Late Cretaceous sedimentary rocks are represented by the Bor Clastics Formation and Oštrej Formation [47]. Deeper parts of the Oštrej Formation exhibit transitions to epiclastic rocks of the Metovnica Formation [48] that is composed of polymictic andesite breccia, volcanoclastic conglomerate and sandstone; the matrix of these sediments often contains reddish marls. The Late Cretaceous volcanic rocks are exclusively represented by andesite of the first phase, which is called ‘Timok andesite’ [48]. However, we recognize two different subgroups of these rocks, which systematically differ in their stratigraphic position and

petrography, and as it will be shown below, in age and in their link to mineralization. These subgroups are hereafter named Timok andesite volcanic phase 1A (V1A) and Timok andesite volcanic phase 1B (V1B).

4.1.1. The Nikoličevo Area

In this section we summarize the stratigraphy of the studied drill-cores from the Nikoličevo area, whereas detailed lithological and petrographic descriptions are given in Supplementary Material 1.

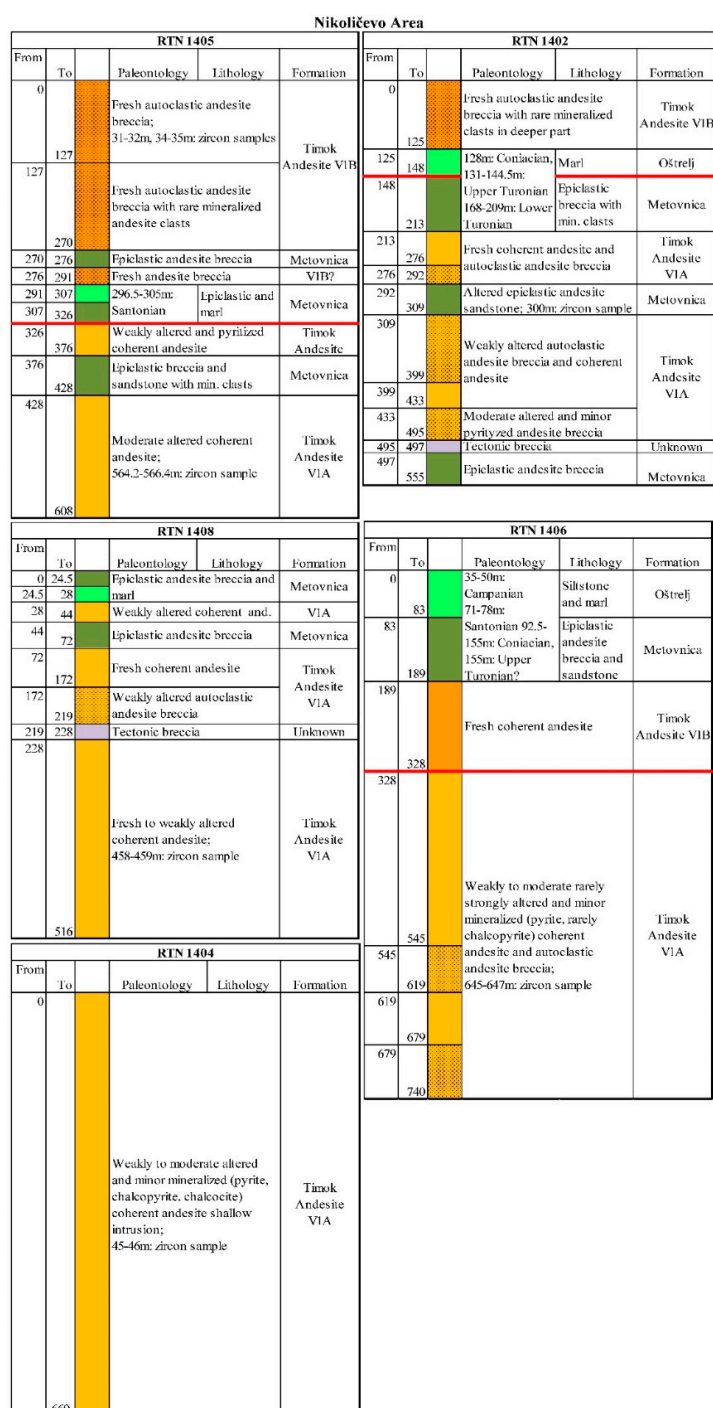


Figure 3. Stratigraphic logs of the drill holes from the Nikoličevo area. The hatched pattern indicates andesite breccia, whereas the red line marks the boundary between the two andesite subgroups.

The entire volcano-sedimentary succession of Nikoličevo can be divided into two stratigraphic horizons. In the upper horizon predominate coherent extrusive facies and/or monomict, autoclastic breccia of fresh andesite V1B; in drill hole RTN 1405, the V1B autoclastic breccia contains rare mineralized andesitic clasts (Figure 5a). The V1B is a fresh andesite rock displaying holo- to hypocrySTALLINE texture and occasionally fluidal fabric. This andesite is characterized by the presence of distinctively large hornblende phenocrysts, commonly several centimeters in length. The hornblende phenocrysts are both coarser and more abundant than phenocrysts of plagioclase, therefore, the V1B can also be named hornblende-plagioclase phyric andesite (Figure 5b,c). The proportion of phenocrysts and microphenocrysts in these rocks is around 50 vol. %. The V1B andesite is both overlain and underlain by laminated grayish siltstones and marls of the Oštrej Formation and is usually underlain by epiclastic rocks of the Metovnica Formation. The available paleontological evidence suggests a Santonian, Lower Turonian to Coniacian age of these sedimentary series (see Table 1). In the lower horizon appear weakly hydrothermally altered and pyritized coherent andesite underlain by a thick series of weakly to moderately altered coherent and autoclastic facies of V1A andesite; between these two V1A sections occur bedded epiclastic rocks that often contain rounded clasts of mineralized andesite (Figure 5d–f). The lowermost parts of drill hole RTN 1402 consist of tectonised epiclastic breccia. In contrast to the V1B, the V1A andesite is plagioclase-hornblende phyric (Figure 5g,h) and has mostly holocrystalline groundmass and a higher proportion of phenocrysts and microphenocrysts (>50 vol. %); in addition, the V1A andesite is substantially altered and mineralized. The drill hole RTN 1404 is specific because it is entirely composed of weakly to moderate hydrothermally altered and poorly mineralized (pyrite, chalcopyrite, chalcocite) coherent shallow intrusive V1A andesite facies (Figure 5i,j). It is worth noting that this drill hole is located along the same direction with Čukaru Peki, although some 5 km towards the east. In addition, westward from Čukaru Peki, along the same line, another shallow intrusive andesite body occurs (a small body of Timok andesite, first volcanic phase—shallow intrusion shown in Figure 2).

Čukaru Peki Area



Figure 4. Stratigraphic logs of two drill holes from the Čukaru Peki area (News Release Reservoir Minerals [21,49]). The hatched pattern indicates andesite breccia, whereas the red line marks the boundary between the two andesite subgroups.

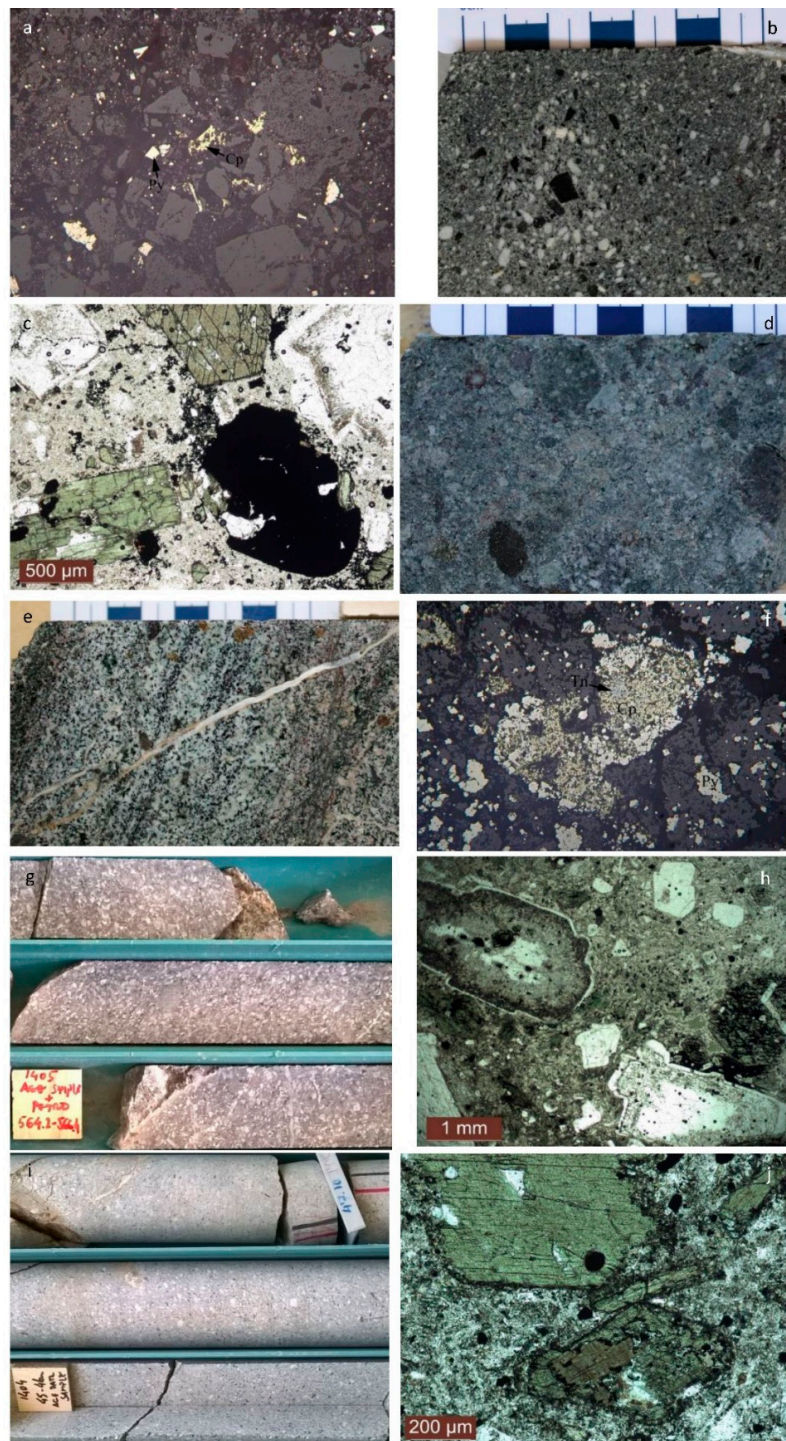


Figure 5. Petrographic characteristics of the studied drill-cores from Nikoličevo: (a) pyrite (Py) and chalcopyrite (Cp) disseminations in rare mineralized clasts in V1B andesitic breccia (reflected light); (b) macroscopic appearance of fresh monomictic, autoclastic andesitic breccia V1B; (c) photomicrograph of andesite V1B (transmitted light, parallel nicols); (d) polymictic epiclastic andesite breccia composed of altered and mineralized clasts of V1A andesite; (e) layered epiclastic sandstone of V1A andesite; (f) photomicrograph of a mineralized V1A andesite clast in epiclastic breccia (reflected light); (g) drill-cores of weakly altered coherent V1A andesite; (h) photomicrograph of weakly-altered V1A andesite (transmitted light, parallel nicols); (i) drill-cores of coherent V1A andesite (shallow intrusion?); (j) photomicrograph of V1A andesite (shallow intrusion?) (transmitted light, parallel nicols); (a–h) drill hole RTN 1405; (i,j) drill hole RTN 1404.

Table 1. Summary on lithological and paleontological characteristics of the studied drill holes. * see ages in Table 2.

Drill Hole Label	Formation	Depth (m)	Lithology and Fossil Record	Age	
RTN 1405	Timok Andesite (V1B)	31–34	Weakly propylitised hornblende andesite breccia	U/Pb*	
		128–262	Hornblende andesite breccia with rare ore (mineralized) clasts		
	Metovnica Epiclastic	296.5–305	Marlstone—biomicrite in epiclastic <i>Globotruncana arca</i> (CUSHMANN), <i>Globotruncana bulloides</i> (VOGLER), <i>Globotruncana lapparenti</i> (BROTZEN), <i>Globotruncana linneiana</i> (d'ORBIGNY), <i>Globotruncana rosseta</i> (CARSEY), <i>Marginotruncana coronata</i> (BOLLI), <i>Marginotruncana marginata</i> (REUSS), <i>Marginotruncana schneegansi</i> (SIGAL), <i>Marginotruncana renzi</i> (GANDOLFI), <i>Contusotruncana fornicata</i> (PLUMMER), <i>Dicarinella asymetrica</i> (SIGAL)—fragment, <i>Globotruncana sp.</i> —fragments, <i>hedbergellas</i> , <i>heterohelicids</i> , <i>globigerinas</i> , <i>globigerinelodes</i> , <i>calcispheres</i> .		Santonian
			Timok Andesite (V1A)	336	Argillitised and minor mineralized (pyrite) hornblende andesite
	Metovnica Epiclastic	396–445	Polymictic andesite sandstone	Fossils not found	
Timok Andesite (V1A)	517–565	Argillitised and propylitised hornblende andesite	U/Pb*		
RTN 1402	Timok Andesite (V1B)	40–42	Hornblende andesite		
	Oštrej	128	Marlstone—biomicrite <i>Globotruncana linneiana</i> (d'ORBIGNY), <i>Marginotruncana coronata</i> (BOLLI), <i>Marginotruncana tarfayaensis</i> (LEHMANN), <i>Marginotruncana pseudolinneiana</i> (ESSAGNO), <i>Marginotruncana sp.</i> , <i>globigerina</i> , <i>globigerinolides</i> , <i>hedbergellas</i> , <i>heterohelicids</i> , <i>calcispheres</i> . group “ <i>Hedbergella-Ticinella</i> ”.		Coniacian
			131–144.5	Marlstone—biomicrite and sandstone <i>Marginotruncana sigali</i> (REICHEL), <i>Marginotruncana tarfayaensis</i> (LEHMANN), <i>Marginotruncana schneegansi</i> (SIGAL), <i>globigerina</i> , <i>rare hedbergellas</i> , <i>heterohelicids</i> , <i>inoceramus</i> .	
	Metovnica Epiclastic	168–209	Sandy marlstone—biomicrite in epiclastic <i>Dicarinella gr. hagni-primitiva</i> , <i>Marginotruncana marginata</i> (REUSS), <i>Globotruncana linneiana</i> (d'ORBIGNY), <i>Marginotruncana sigali</i> (REICHEL), <i>Marginotruncana schneegansi</i> (SIGAL), <i>Marginotruncana paraconavata</i> (PORTHAULT), <i>Marginotruncana pseudolinneiana</i> (PESSAGNO), <i>Praeglobotruncana cf. stephani</i> (GANDOLFI), <i>Rotalipora sp.</i> —fragments, <i>Marginotruncana sp.</i> , <i>Dicarinella sp.</i> , <i>Whiteinella sp.</i> , <i>heterohelicids</i> , <i>globigerinolides</i> , group “ <i>Hedbergella-Ticinella</i> ”.		Lower Turonian
			297–306	Zeolitized polymictic andesite sandstone	Fossils not found
Timok Andesite (V1A)	483	Argillitised to propylitised, minor mineralized (pyrite) hornblende andesite breccia			
Metovnica Epiclastic	515–540	Sandstone and siltstone in epiclastic	Fossils not found		

Table 1. Cont.

Drill Hole Label	Formation	Depth (m)	Lithology and Fossil Record	Age
RTN 1406	Oštrej	11	Sandstone—arkose Fossils not found	
		35–50	Marlstone—biomicrite <i>Globotruncana arca</i> (CUSHMAN), <i>Globotruncana lapparenti</i> (BROTZEN), <i>Globotruncana linneiana</i> (d'ORBIGNY), <i>Globotruncana hilli</i> (PESSAGNO), <i>Globotruncana cf. ventricosa</i> (WHITE), <i>Contusotruncana fornicata</i> (PLUMMER), <i>Marginotruncana coronata</i> (BOLLI), <i>Globotruncana sp.</i> —fragments, <i>hedbergellas</i> , <i>heterohelicids</i> , <i>globigerina</i> , <i>calcispheres</i> .	Campanian
		71–78	Marlstone—biomicrite <i>Contusotruncana fornicata</i> (PLUMMER), <i>Marginotruncana renzi</i> (GANDOLFI), <i>Marginotruncana schneegansi</i> (SIGAL), <i>Marginotruncanatarfayaensis</i> (LEHMANN), <i>Marginotruncana marginata</i> (REUSS), <i>Globotruncana lapparenti</i> (BROTZEN), <i>Globotruncana bulloides</i> (VOGLER), <i>Globotruncana hilli</i> (PESSAGNO), <i>Globotruncana linneiana</i> (d'ORBIGNY), <i>globigerina</i> , <i>hedbergellas</i> , <i>calcispheres</i> , <i>heterohelicids</i> .	Santonian
	Metovnica Epiclastic	92.5–121	Marlstone—biomicrite in epiclastic <i>Globotruncana lapparenti</i> (BROTZEN), <i>Globotruncana linneiana</i> (d'ORBIGNY), <i>arginotruncana coronata</i> (BOLLI)—fragments, <i>globigerina</i> , <i>hedbergellas</i> , <i>heterohelicids</i> , <i>calcispheres</i> , <i>globigerinoides</i> .	Coniacian
		155	Marlstone—fossiliferous micrite (mudstone) in epiclastic <i>Marginotruncana coronata</i> (BOLLI)—deformed, <i>Marginotruncana renzi</i> (GANDOLFI), <i>Dicarinella primitiva</i> (DALBIEZ), <i>globigerina</i> , <i>hedbergellas</i> , <i>heterohelicids</i> , <i>calcispheres</i> .	Upper Turonian-Coniacian
		Timok Andesite (V1B)	195	Hornblende andesite
	Timok Andesite (V1A)	328–729	Argillitised to propylitised and minor mineralized (pyrite, rare chalcopyrite) hornblende andesite and andesite breccia	U/Pb*
RTN 1408	Timok Andesite (V1A)	458–459	Propylitised hornblende andesite	U/Pb*
RTN 1404	Timok Andesite (V1A)	45–666	Argillitised to propylitised and minor mineralized (pyrite, chalcopyrite, chalcocite) hornblende andesite	U/Pb*

4.1.2. The Čukaru Peki Area

The general geology of the Čukaru Peki area is illustrated by drill holes FMTC1335 and FMTC1213 (see Figure 4). The cover is represented by clastic Miocene sediments that overlie a Late Cretaceous volcano-sedimentary series composed of three different packages. The uppermost package is composed of coarse-grained clastic sediments of the so-called Bor Clastics Formation. The other two packages consist of grayish siltstones and marls of the Oštrej Formation, which are underlain by a series of interlayered reddish marls and epiclastics of the Metovnica Formation. The epiclastics are composed of polymictic andesite breccia that often contain reddish marls in the matrix.

The entire Late Cretaceous sedimentary series of these two Čukaru Peki drill holes is neither mineralized nor hydrothermally altered and it seals the mineralization. The series is immediately underlain by unaltered coherent and autoclastic facies of the V1B andesite. Below the V1B horizon

occurs a thick series (~1000 m in the drill hole FMTC1335) of coherent to brecciated volcanic facies that show very similar petrography to the above described V1A andesite from the Nikoličevo drill holes. In drill hole FMTC1213, the mineralization is represented by massive, high-sulphidation epithermal mineralization of copper and gold. Intense mineralization of massive pyrite, covellite, enargite, and locally bornite mainly occurs as replacements, fine-grained disseminations, breccia matrix fill and veinlets in strongly quartz-alunite (typical advanced argillic alteration type)-altered brecciated andesite. The intervals with the highest copper grades consist of more than 90% of sulphide minerals. They comprise 160.0 m with an average grade of 6.92% Cu and 5.40 g/t Au. Deeper parts of the drill hole (from 633 m) consist of brecciated andesite with a lower intensity of alteration and sulphide mineralization. In generally the same stratigraphic position in FMTC1335 appears Cu–Au porphyry type of mineralization with chalcopyrite as a predominant copper mineral. The mineralization also contains pyrite, locally molybdenite, bornite, magnetite and hematite and is hosted by a strongly propylitised andesite, with anhydrite-gypsum veins. The richest mineralization interval is 471.6-m thick with an average grade of 0.41% Cu and 0.22 g/t Au (provided by News Release Reservoir Minerals [21,49]).

4.2. U/Pb Geochronology

The geochronological investigations include seven new U/Pb zircon analyses from the studied drill holes of the Nikoličevo area. The final age data are given in Table 2, whereas the full data set is provided as Supplementary Material 2. First, we used the concordia diagram (Supplementary Material 2) in order to exclude all discordant data from the calculation, whereas in the second step we calculated the mean $^{206}\text{Pb}/^{238}\text{U}$ average age. The obtained new results are plotted in Figures 6 and 7.

Both hornblende andesite breccias show similar U/Pb ages at 84.89 ± 0.75 Ma (RTN 1405, 31–32 m) and 85.56 ± 0.53 Ma (RTN 1405, 34–35 m). All other obtained U/Pb age data (RTN 1405, 564.2–566.4 m; RTN 1402, RTN 1404, RTN 1408, RTN 1406) are scattering between 89.49 ± 0.42 Ma and 90.97 ± 0.39 Ma (Figures 6 and 7). An average age of the younger group, hornblende-plagioclase phyric andesite, is 85.23 ± 0.47 Ma, which clearly separates this andesite from the older group, plagioclase-hornblende phyric andesite with an average age of 90.05 ± 0.61 Ma.

Table 2. U/Pb zircon ages of samples of V1A and V1B andesite units from Nikoličevo. The ages are calculated as weighted $^{206}\text{Pb}/^{238}\text{U}$ mean values.

Drill Hole	Depth (m)	Lab. No	Lithology	Age Ma
RTN 1405	31–32	Avq. 380	Hornblende-plagioclase phyric andesite breccia (V1B)	84.89 ± 0.75
RTN 1405	34–35	Avq. 383	Hornblende-plagioclase phyric andesite breccia (V1B)	85.56 ± 0.53
RTN 1405	564.2–566.4	Avq. 381	Plagioclase-hornblende phyric andesite (V1A)	89.49 ± 0.42
RTN 1402	300.5–301.5	Avq. 375	Andesite clast from zeolitized epiclastic sandstone (V1A)	89.80 ± 0.56
RTN 1404	45–46	Avq. 377	Weakly propylitised and mineralized plagioclase-hornblende phyric andesite (V1A)	89.64 ± 0.51
RTN 1408	458–459	Avq. 374	Weakly propylitised plagioclase-hornblende phyric andesite (V1A)	90.37 ± 0.66
RTN 1406	645–647	Avq. 378	Weakly propylitised plagioclase-hornblende phyric andesite (V1A)	90.97 ± 0.39

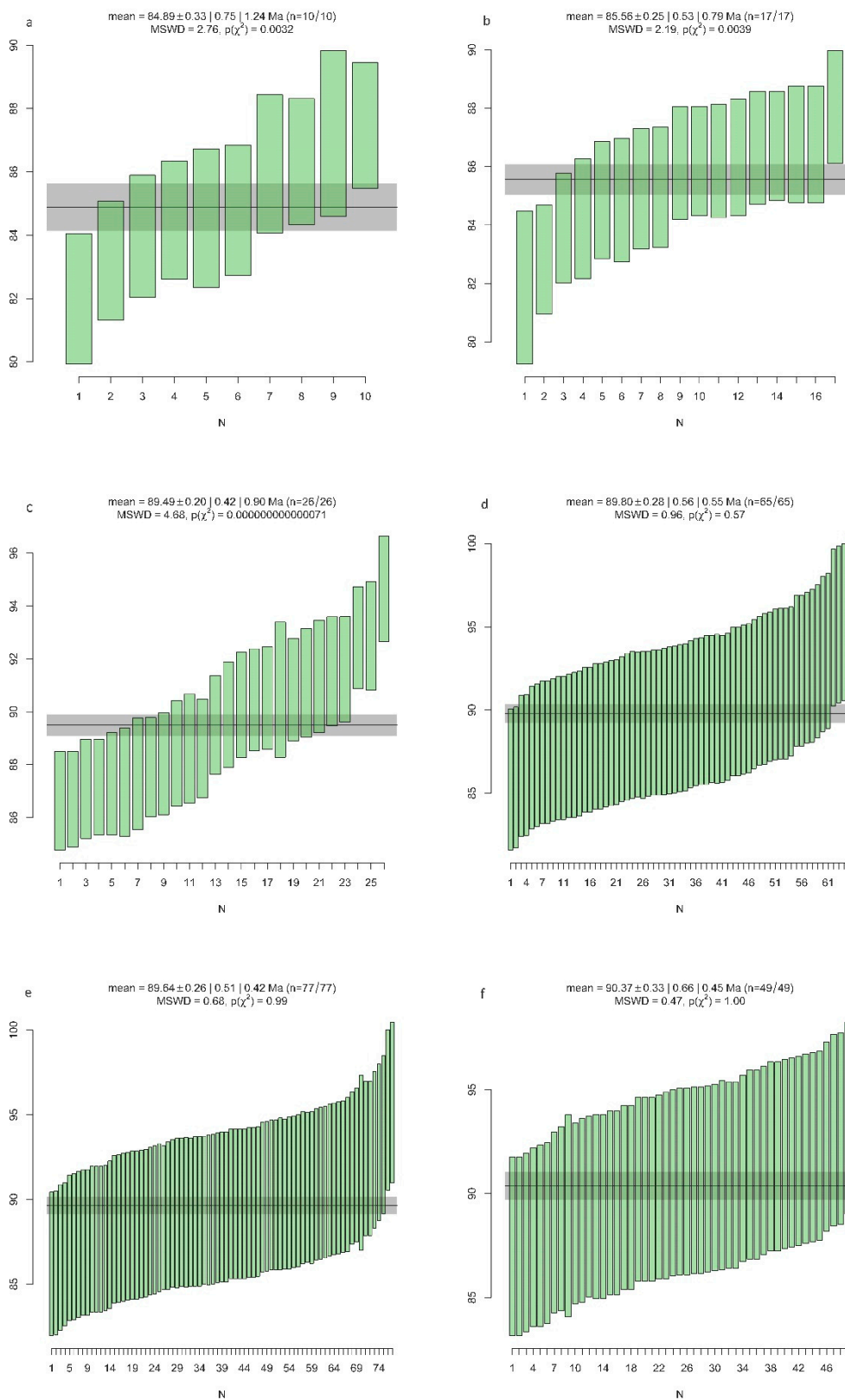


Figure 6. Cont.

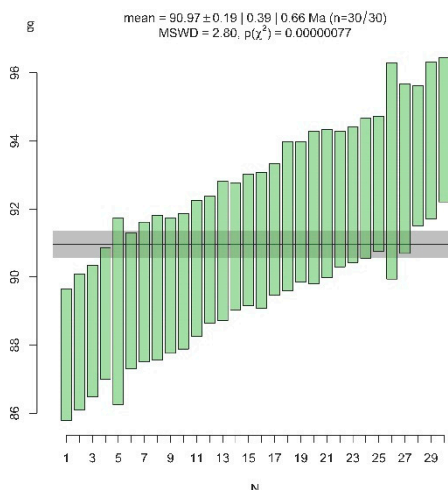


Figure 6. The new obtained weighted mean $^{206}\text{Pb}/^{238}\text{U}$ data. The raw data are available in Supplementary Material 2. (a–c) drill hole RTN 1405; (d) drill hole RTN 1402; (e) drill hole RTN 1404; (f) drill hole RTN 1408; (g) drill hole RTN1406.

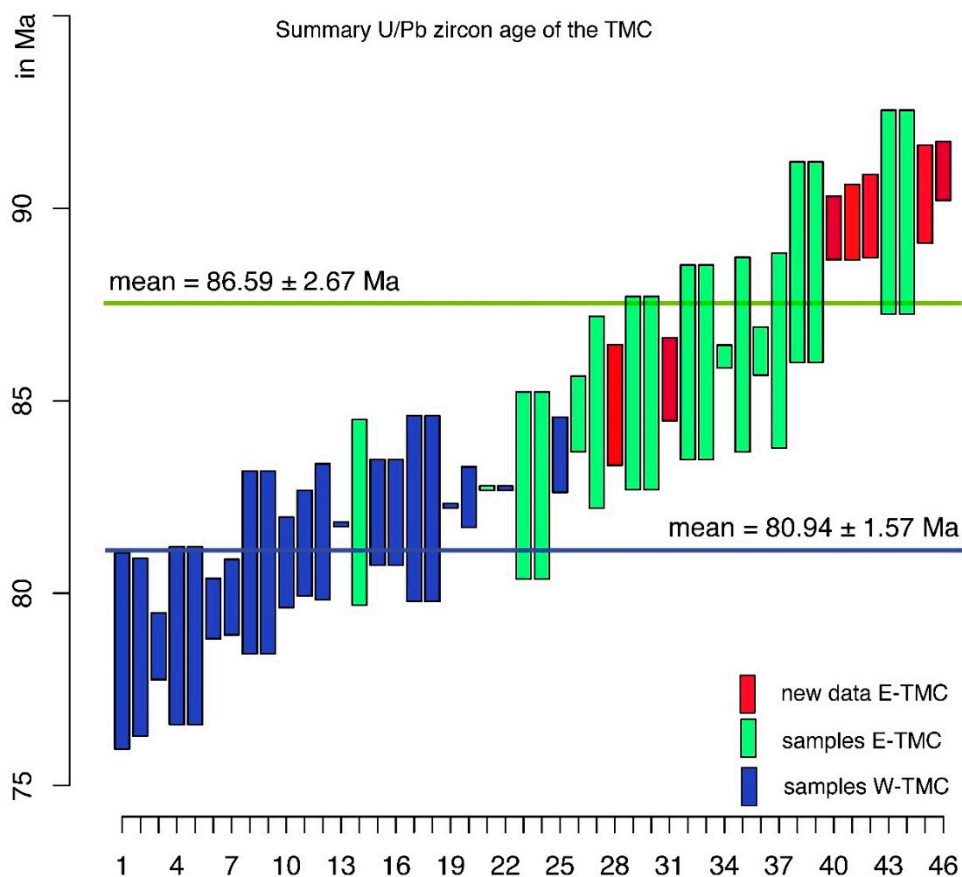


Figure 7. Summary plot of U/Pb zircon data of the TMC, including our new data set. The blue and red colours represent ages of the west- and east-TMC, respectively, whereas our new data set is plotted in red [7,11,13,32]. The individual analyses showing 2 sigma errors and new average age calculation of the East and West is 1SD error.

5. Discussion

The observations and data resulting from the investigations of the logs from Nikoličevo (and Čukaru Peki), allow us, first, to distinguish two subgroups among the first phase andesites, and second, to use their petrological differences in order to derive new implications on the link between magmatism and metallogeny. Note that we provide our arguments by investigating extrusive volcanic facies instead of intrusions; namely, in line with previous studies (e.g., [8,9,13,17–19,25,34,50]), we argue that the occurring volcanic rocks sufficiently reflect the fertility of their non-exposed intrusive counterparts.

5.1. Two Subgroups of the 1st Phase Andesite in the BMZ

In spite of the fact that our study addresses a relatively small part of the BMZ, the reported stratigraphic and petrographic observations and new U/Pb radiometric data enable us to conclude that the first volcanic phase in the BMZ must have occurred during at least two different volcano-intrusive events. As already explained, we named the volcanic products of these two magmatic events, V1A (older) and V1B (younger) andesite. The new data (Figure 6) show that the V1A and V1B andesite subgroups display different emplacement ages, stratigraphic positions and petrographic characteristics.

The V1A andesite is logged in the lower sections of the studied drill holes and is predominantly represented by altered and sometimes heavily mineralized rocks. These volcanics are coarsely porphyritic with holocrystalline (glass-free) groundmass and with the relative number of phenocrysts higher than 50% vol. In this andesite plagioclase, phenocrysts predominate over hornblende phenocrysts and microphenocrysts, both in size and in relative abundance. The V1A andesite is radiometrically dated in several drill holes of Nikoličevo, revealing an age range of 89.3–90.9 Ma; this range is roughly consistent with previously obtained U/Pb ages for andesites of the easternmost part of the Timok Magmatic Complex ([11,32] see Figure 7).

The V1B andesite facies occupy upper sections of almost all the studied logs. They are often found in contact with Coniacian to Campanian silty and marly sediments or younger epiclastics containing reddish marly material in the matrix. The V1B part of the volcanic succession is missing in RTN 1404 and 1408 drill holes (see Figure 3), most likely due to subsequent removal by erosion. In contrast to the V1A, the V1B andesite is hornblende-plagioclase phyric with holo- to hypocrySTALLINE groundmass and a lower phenocrysts/matrix ratio. The V1B rocks from the drill hole RTN 1405 are radiometrically dated, revealing ages of 84.89 ± 0.78 Ma and 85.23 ± 0.56 Ma. These ages are overlapping those obtained on petrographically very similar hornblende-plagioclase phyric andesite that are exposed in the large Veliki Krivelj porphyry copper deposit (84.66 ± 0.5 Ma; [32]). The stratigraphic separation between the V1A and V1B subgroups is made according to the characteristics shown by their primary volcanic facies, i.e., coherent lavas and non-reworked autoclastic deposits. On the other hand, polymictic epiclastic deposits, occurring in various stratigraphic positions in the investigating drill holes, were not used for this purpose, because they usually contain fragments of both V1A and V1B andesite. In drill hole RTN 1405, in the bottom parts of the V1B (primary?) autoclastic breccia rare mineralized andesitic clasts are observed (see Figure 5a); although the primary volcanic texture of these fragments has been obliterated, it is supposed that they represent fragments of V1A andesite, which were accidentally incorporated into the V1B autoclastic lava.

The existence of the V1A and V1B andesite subgroups is also evident from the stratigraphy of two drill holes from the Čukaru Peki area (Figure 4). These two types of andesite are even more petrographically different in these drill holes, because they are situated closer to the main ore bodies of Čukaru Peki deposit. Hence, the V1A andesite from the lower log sections is strongly altered and mineralized by high sulphidation massive Cu–Au ore and/or porphyry disseminations, whereas on top of these logs, almost-fresh V1B andesite appears. All available U/Pb ages are plotted in Figures 6 and 7; the obtained U/Pb data set distinguishes two groups, the west- and the east-TMC; these groups show age ranges from 82.10 Ma to 90.97 Ma (east-TMC) and from 78.50 Ma to 83.60 Ma (west-TMC) with an average age of 86.59 Ma and 80.94 Ma, respectively.

In summary, the presented observations and the U/Pb radiometric data argue that the volcanic rocks of the first phase are heterogeneous and can be distinguished according to their stratigraphic position, age and petrography. This has at least two implications. First, the collective term ‘Timok andesite’ does not apply anymore; it is particularly important because the previous interpretations invoke that this entire group is petrogenetically related to ore forming processes. Second, the half-a-century-old three-phase interpretation of magmatic evolution of the TMC/BMZ should be re-examined; namely, the possibility that this complex developed through continuous magmatic activity over a time span from >90 Ma to 70 Ma (including the Ridanj-Krepoljin Zone further in the west) must be taken into account.

5.2. The Main Mineralization Event in the BMZ Revisited

The most reliable constrains of the time of mineralization in the BMZ are the ages obtained by Re-Os method in molybdenite [10]; the age of 87.88 Ma (Veliki Krivelj) does not overlap with U/Pb zircon ages of 86.17 Ma (post-ore) and 86.29 Ma (syn-ore) [33], whereas the Re-Os age of 86.09 Ma (σ of 2 data) of Bor is close to the data set from Veliki Krivelj; six Re-Os ages of the Majdanpek ore with an average age range of 83.52 Ma overlap very well with U/Pb zircon ages (84.4–83.6 Ma syn-ore and 83.2 Ma–82.8 Ma post-ore) of the magmatic rocks of Majdanpek [51].

Our results and interpretation suggest that the ore-forming process in the Nikoličevo and the Čukaru Peki area occurred roughly simultaneously to those at Bor and Veliki Krivelj or are even slightly older. The mineralization event at Nikoličevo and Čukaru Peki was likely contemporaneous to V1A magmatism in this area, which gave an age of 89–90 Ma. The possibility that mineralization is younger, i.e., that the V1A andesite was altered and mineralized by later hydrothermal episodes cannot be excluded, but these processes must have occurred before the emplacement of the V1B, i.e., before 85–86 Ma. This is evident from the observation that the V1B andesite is fresh and barren even when found in direct contact with the underlying V1A rocks; this is documented in the drill holes RTN 1406 and FTMC1335 at Nikoličevo and Čukaru Peki, respectively.

Accordingly, the areas of Nikoličevo and Čukaru Peki host two compositionally similar andesite subgroups that exhibit sharply different ore productivity; therefore, they are perfect sites for studying the interplay between magmatism and Cu–Au metallogeny. The first-order result of our study suggests that the main mineralization event was genetically related to the emplacement of plagioclase-hornblende phyric holocrystalline V1A andesite porphyry.

As already mentioned, the entire first phase andesite has always been considered a single rock group collectively named ‘Timok andesite’. For example, Kolb, et al. [11] argued that these rocks show an adakitic affinity expressed by high Sr/Y values and low Y and HREE contents [52,53]. It is generally known that the adakite affinity is commonly present in andesite/diorite rocks associated with porphyry-epithermal systems (e.g., [54–56]). The previous studies suggest that the Timok andesites acquired their adakitic geochemical signature via AFC (assimilation-fractional crystallization) processes in which high-pressure accumulation of amphibole had played an important role [11]. A similar scenario for obtaining adakitic compositional signature, which involves hornblende (\pm garnet) fractionation of mafic to intermediate melts in the lower crustal levels, is suggested for other active margin regions known for hosting large Cu–Au porphyry-epithermal systems ([57–60], among others).

Assuming that the hypothesis suggested by [11] is correct, namely that hornblende-dominated fractionation was responsible for adakitic geochemical characteristics and thereby for the high mineralizing potential of Timok andesites, we suppose that the observed contrasting productivities of the V1A and V1B andesite may have been the result of small disturbances during the proposed AFC processes. We also argue that these fluctuations may have been at least partly evidenced from the change in the order of crystallization of hornblende and plagioclase, shown by the V1A and V1B andesite.

In order to explain our idea more in detail, we need first to recall a general model of the formation of Cu–Au productive andesite magmas (see [61] and references therein). The model involves the formation of primary mafic/intermediate melts initially enriched in volatiles, in particular water

(>4 wt. %), sulphur and chlorine, which are also characterized by elevated oxygen fugacity, commonly 1 or 2 above the QMF (quartz-magnetite fayalite) buffer (e.g., [62–64]). These primary melts usually form in subduction zones, but they are also known to occur in post-collisional settings.

The critical point of our interpretation is the fractionation of primary/parental basic to intermediate magmas, during which hornblende appears early in the crystallization sequence, likely in deep crustal levels (e.g., [65–68]). The stabilization field of hornblende in water-rich melts is enlarged at the expense of the stability of plagioclase [69–71]. As already mentioned above, this is an explanation of how evolved magmas acquire adakitic geochemical characteristics [57]. Upon reaching shallower crustal levels, the still evolving magma with adakite signature may either erupt and/or emplace as andesite/diorite porphyry or, alternatively, may reside longer in the shallow crust. In case of pre-mature decompression, the evolving magma becomes saturated with volatiles via so-called “first boiling” [72], and that decreases the capacity of hornblende-plagioclase phyric andesite to produce hydrothermal events. By contrast, in the case of prevented decompression ($P > 1\text{--}2$ kb), hornblende ceases to precipitate and accumulate, and the separated melt continues to preferentially crystallize plagioclase. By advanced crystallization of plagioclase in such shallow magmatic chambers, i.e., under post-emplacement conditions, the remaining melt becomes extremely enriched in volatiles, which induces ‘second boiling’ and the formation of a powerful hydrothermal system (e.g., [73,74]).

Although our model does not address many other factors controlling magma fertility, such as high sulphur and/or chlorine contents as well as high oxygen fugacity (see [75] and references therein), it indicates that the V1B andesite magmatism was not productive because the fractionation (\pm assimilation) of its parental magma had been interrupted before the evolving melt reached the moment of the switch in the crystallization sequence between hornblende and plagioclase. The hornblende-plagioclase phyric V1B magma emplaced (decompressed) too early for second boiling; the lower proportion of phenocrysts and the presence of glass in the groundmass of the V1B andesite support such a scenario. By contrast, slightly more evolved V1A melts resided longer in shallow crustal levels; therefore, they extensively precipitated plagioclase, which is indeed observed as the most abundant phenocryst and microphenocrysts phase in these rocks. The advanced crystallization of plagioclase induced an increase of water contents in the final liquid and preconditioned the formation of a hydrothermal system. The main reasoning for this interpretation is summarized and illustrated in a simplified sketch in Figure 8.

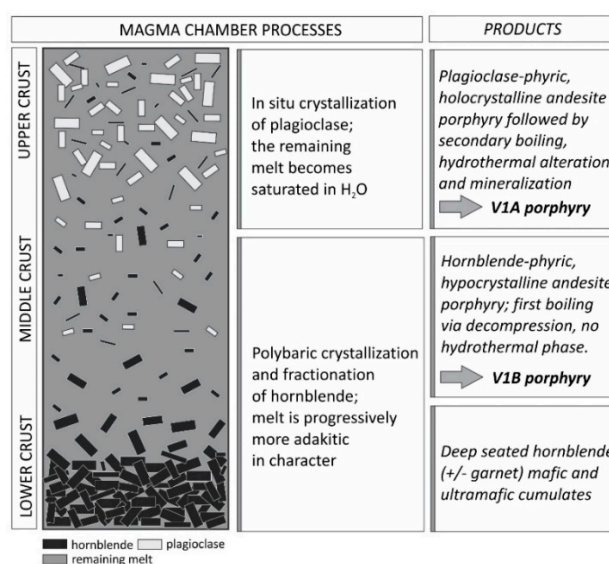


Figure 8. Not-to-scale sketch illustrating polybaric fractional crystallization of a mafic/intermediate magma initially rich in water, sulphur, chlorine and characterized by high oxygen fugacity; on the right-hand side, depth-dependent crystallization sequences are described.

The scenario of early decompression and first boiling is also considered as an explanation for the low ore productivity shown by the second volcanic phase in the BMZ. The second phase products are represented by less crystallized and less evolved andesites (\pm basaltic andesites) which predominantly formed in the west of the BMZ, simultaneously with rifting and the formation of large depositional environments. Accordingly, these magmas may have reached eruption/emplaced levels earlier, due to a higher extension rate in this area.

Although our interpretation still waits to be tested with additional analytical data, it surely sheds new light onto the Late Cretaceous magmatic and metallogenetic processes in the BMZ. In this context, we emphasize that thorough field and petrographic observations are very important for prospecting even in the areas with long-standing exploration and exploitation.

6. Conclusions

By studying drill holes of Nikoličevu and by the correlation of the obtained data with the information available from the recently discovered Čukaru Peki deposit, we postulate the following conclusions:

1. The oldest, first phase andesite ('Timok andesite') occurs in the easternmost part of the BMZ, along with the major Cu–Au porphyry and epithermal ore deposits; newly obtained U/Pb zircon ages of these rocks reveal an age range of 85–90 Ma, which roughly overlaps with the earlier estimates.
2. We presented evidence that the first phase andesite consists of two subgroups; the older V1A andesite (~89–90 Ma) is both in time and space associated to the ore mineralization, whereas the younger V1B (~85–86 Ma) postdates the main mineralization event.
3. Subtle petrographic differences between the V1A and V1B andesite may be used for explaining their different ore productivity; our simplified petrogenetic model involves the fractionation of water-rich parental (primary?) melts; it is supposed that an early decompression event that occurs before the evolving melt reaches the stability field of plagioclase in water-rich magma prevents second boiling and thereby critically lowers the ore productivity of magma.
4. The study strongly underlines that the results of routine field and petrographic observations should be used as important prospection criteria.

Supplementary Materials: The following are available online at <http://www.mdpi.com/2075-163X/9/11/672/s1>.

Author Contributions: Conceptualization of the study: M.B. and V.C.; overall design of the methodology: V.C. and A.v.Q.; U/Pb data acquiring and validation: A.v.Q. and I.P.; petrographic analysis: M.B., V.C. and A.P.; sedimentological and paleontological study: N.V. and D.L.O.; writing—original draft preparation, V.C.; writing—review and editing, V.C., M.B. and A.P.; visualization, M.B., V.C. and A.v.Q.; funding acquisition, M.B.; zircon CL images, I.P.

Funding: The study was funded by projects no. 176016 of the Ministry of Education, Science and Technological Development of the Republic of Serbia, nos. F9 and F17 of the Serbian Academy of Sciences and Arts, and no. IZ74ZO_160512 (SCOPES) of Swiss National Science Foundation.

Acknowledgments: We are grateful to Jocelyn McPhie for their helpful suggestions which improved the manuscript. We would also like to thank all the colleagues for constructive help. Three reviewers are kindly acknowledged for constructive comments and suggestions.

Conflicts of Interest: The authors declare no conflict of interest.

References

1. Berza, T.; Constantinescu, E.; Serban-Nicolae, V. Upper Cretaceous Magmatic Series and Associated Mineralisation in the Carpathian-Balkan Orogen. *Resour. Geol.* **1998**, *48*, 291–306. [[CrossRef](#)]
2. von Quadt, A.; Moritz, R.; Peytcheva, I.; Heinrich, C. Geochronology and geodynamics of Late Cretaceous magmatism and Cu–Au mineralization in the Panagyurishte region of the Apuseni-Banat-Timok-Srednogie belt, Bulgaria. *Ore Geol. Rev.* **2005**, *27*, 95–126. [[CrossRef](#)]
3. Janković, S. The Copper Deposits and Geotectonic Setting of the Tethyan Eurasian Metallogenetic Belt. *Miner. Depos.* **1977**, *12*, 37–47. [[CrossRef](#)]

4. Patrascu, S.; Bleahu, M.; Panaiotu, C. Tectonic implications of paleomagnetic research into Upper Cretaceous magmatic rocks in the Apuseni Mountains, Romania. *Tectonophysics* **1990**, *180*, 309–322. [[CrossRef](#)]
5. Patrascu, S.; Panaiotu, C.; Seclaman, M.; Panaiotu, B. Timing of rotational motion of Apuseni Mountains (Romania): Paleomagnetic data from Tertiary magmatic rocks. *Tectonophysics* **1994**, *233*, 163–176. [[CrossRef](#)]
6. Marton, E.; Tischler, M.; Csontos, L.; Fuegenschuh, B.; Schmid, S.M. The contact zone between the ALCAPA and Tisza-Dacia megatectonic units of Northern Romania in the light of new paleomagnetic data. *Swiss J. Geosci.* **2007**, *100*, 109–124. [[CrossRef](#)]
7. Banješević, M.; Cvetković, V.; Koželj, D.; Peytcheva, I.; von Quadt, A. The Timok Magmatic Complex and Ridan Krepoljin Zone: Geodynamical Evolution. In Proceedings of the International Symposium – Geology and metallogeny of copper and gold deposits in the Bor Metallogenic zone – Bor 100 years, Bor Lake, Yugoslavia, 24–25 October 2002; Koželj, D., Jelenković, R., Eds.; RTB Bor Holding Company: Bor, Serbia, 2002; pp. 199–202.
8. Clark, A.H.; Ullrich, T.D. ⁴⁰Ar/³⁹Ar age data for andesitic magmatism and hydrothermal activity in the Timok Massif, eastern Serbia: Implications for metallogenetic relationships in the Bor copper-gold subprovince. *Miner. Depos.* **2004**, *39*, 256–262. [[CrossRef](#)]
9. Lips, A.; Herrington, R.; Stein, G.; Koželj, D.; Popov, K.; Wijbrans, J. Refined timing of porphyry copper formation in the Serbian and Bulgarian portions of the Cretaceous Carpatho–Balkan Belt. *Econ. Geol.* **2004**, *99*, 601–609. [[CrossRef](#)]
10. Zimmerman, A.; Stein, H.; Hannah, J.; Koželj, D.; Bogdanov, K.; Berza, T. Tectonic configuration of the Apuseni–Banat–Timok–Srednogorie Belt, Balkans–South Carpathians, constrained by high precision Re–Os molybdenite ages. *Miner. Depos.* **2008**, *43*, 1–21. [[CrossRef](#)]
11. Kolb, M.; von Quadt, A.; Peytcheva, I.; Heinrich, C.A.; Fowler, S.J.; Cvetković, V. Adakite-Like and Normal Arc Magmas: Distinct fractionation paths in the East Serbian segment of the Balkan Carpathian Arc. *J. Petrol.* **2013**, *54*, 421–451. [[CrossRef](#)]
12. Gallhofer, D.; von Quadt, A.; Peytcheva, I.; Schmid, S.M.; Heinrich, C.A. Tectonic, magmatic, and metallogenic evolution of the Late Cretaceous arc in the Carpathian-Balkan orogeny. *Tectonics* **2015**, *34*, 1813–1836. [[CrossRef](#)]
13. Knaak, M.; Marton, I.; Tosdal, R.M.; Van der Toorn, J.; Davidović, D.; Strmbanović, I.; Zdravković, M.; Živanović, J.; Hasson, S. Geologic Setting and Tectonic Evolution of Porphyry Cu–Au, Polymetallic Replacement, and Sedimentary Rock-Hosted Au Deposits in the Northwestern Area of the Timok Magmatic Complex, Serbia. *Soc. Econ. Geol. Inc. Spec. Publ.* **2016**, *19*, 1–28.
14. von Quadt, A.; Peytcheva, I.; Kamenov, B.; Fanger, L.; Heinrich, C.A.; Frank, M. The Elatsite porphyry copper deposit in the Panagyurishte ore district, Srednogorie zone, Bulgaria: U–Pb zircon geochronology and isotope-geochemical investigations of magmatism and ore genesis. In *The Timing and Location of Major ore Deposits in an Evolving Orogen*; Blundell, D.J., Neubauer, F., von Quadt, A., Eds.; Spec. Publication 204; Geological Society: London, UK, 2002; pp. 81–102.
15. von Quadt, A.; Peytcheva, I.; Heinrich, C.; Cvetković, V.; Banješević, M. Upper Cretaceous magmatic evolution and related Cu–Au mineralization in Bulgaria and Serbia. In Proceedings of the 9th Biennial SGA Meeting—Mineral Exploration and Research: Digging Deeper, Dublin, Ireland, 20–23 August 2007; Andrew, C.J., Ed.; Society for Geology Applied to Mineral Deposits: Geneva, Switzerland, 2007; pp. 861–864.
16. Janković, S. Metallogenic features of copper deposits in the volcanointrusive complexes of the Bor district, Yugoslavia. In *Monograph European Copper Deposits*; Janković, S., Sillitoe, R.H., Eds.; Society of Economic Geologists, Faculty of Mining and Geology: Belgrade, Serbia, 1980; pp. 42–49.
17. Janković, S. Types of copper deposits related to volcanic environment in the Bor district, Yugoslavia. *Geol. Rundsch.* **1990**, *79*, 467–478. [[CrossRef](#)]
18. Koželj, D. *Epithermal Gold Mineralization in the Bor Metallogenic Zone: Morphogenetic Types, Structural-Texture Varieties and Potentiality*; Special Edition; Copper Institute: Bor, Serbia, 2002. (In Serbian)
19. Jelenković, R.; Milovanović, D.; Koželj, D.; Banješević, M. The Mineral Resources of the Bor Metallogenic Zone: A Review. *Geol. Croat.* **2016**, *69*, 143–155. [[CrossRef](#)]
20. Zijin Mining Group Co. Ltd. Available online: <http://www.zijinmining.com/business/product-detail-47444.htm> (accessed on 12 March 2019).
21. Reservoir Minerals Inc. Available online: <https://www.marketscreener.com/RESERVOIR-MINERALS-INC-15252875/news/> (accessed on 16 July 2019).

22. Banješević, M.; Large, D. Geology and mineralization of the new copper and gold discovery south of Bor—Timok Magmatic Complex. In Proceedings of the XVI Serbian Geological Congress, Donji Milanovac, Serbia, 22–25 May 2014; Cvetković, V., Ed.; Serbian Geological Society: Belgrade, Serbia, 2014; pp. 739–740.
23. Arribas, A., Jr. Characteristics of high-sulfidation epithermal deposits, and their relation to magmatic fluid. In *Magmas, Fluids, and Ore Deposits*; Thompson, J.F.M., Ed.; Mineralogical Association of Canada: Victoria, BC, Canada, 1995; pp. 419–454.
24. Hedenquist, J.W.; Arribas, A., Jr. Evolution of an Intrusion-Centered Hydrothermal System: Far Southeast-Lepanto Porphyry and Epithermal Cu-Au Deposits, Philippines. *Econ. Geol.* **1997**, *93*, 373–404. [[CrossRef](#)]
25. Armstrong, R.; Koželj, D.; Herrington, R. The Majdanpek Porphyry Cu-Au Deposit of Eastern Serbia: A Review. In *Super Porphyry Copper & Gold Deposits—A Global Perspective*; Porter, T.M., Ed.; PGC: Adelaide, Australia, 2005; pp. 453–466.
26. Schmid, S.M.; Bernoulli, D.; Fügenschuh, B.; Matenco, L.; Schefer, S.; Schuster, R.; Tischler, M.; Ustaszewski, K. The Alpine-Carpathian-Dinaridic orogenic system: Correlation and evolution of tectonic units. *Swiss J. Geosci.* **2008**, *101*, 139–183. [[CrossRef](#)]
27. Karamata, S.; Knežević, V.; Pécskay, Z.; Đorđević, M. Magmatism and metallogeny of the Ridanj–Krepoljin belt (eastern Serbia) and their correlation with northern and eastern analogues. *Miner. Depos.* **1997**, *32*, 452–458. [[CrossRef](#)]
28. Banješević, M. The volcanic rocks petrology and K/Ar ages for wide zone Bor ore deposit as part of the Timok magmatic complex (east Serbia). In Proceedings of the ABCD GEODE Workshop, Vata Bai, Romania, 8–12 June 2001; Geological Institute of Romania: Bucharest, Romania, 2001; pp. 39–40.
29. Banješević, M.; Cocić, S.; Radović, M. Petrology and K/Ar ages of volcanic rocks for wide Bor zone as the part of the Timok Magmatic Complex (East Serbia). *Rev. Roum. Geol.* **2002**, *46*, 47–60.
30. Banješević, M.; Cvetković, V.; von Quadt, A.; Peytcheva, I.; Cocić, S. Geodynamic reconstructions based of the magmatism in the Timok Magmatic Complex (East Serbia)—Part of the Carpathian-Balkan belt. In Proceedings of the XVIII Congress of CBGA, Belgrade, Serbia, 3–6 September 2006; Sudar, M., Ercegovic, M., Grubić, A., Eds.; Serbian Geological Society: Beograd, Serbia, 2006; pp. 27–29.
31. Cvetković, V.; Šarić, K.; Prelević, D.; Genser, J.; Neubauer, F.; Höck, V.; von Quadt, A. An anorogenic pulse in a typical orogenic setting: The geochemical and geochronological record in the East Serbian latest Cretaceous to Palaeocene alkaline rocks. *Lithos* **2013**, *180–181*, 181–199. [[CrossRef](#)]
32. von Quadt, A.; Peytcheva, I.; Cvetković, V.; Banješević, M.; Koželj, D. Geochronology, geochemistry and isotope tracing of the Cretaceous magmatism of East-Serbia as part of the Apuseni-Timok-Srednogie metallogenic belt. *Geol. Carpathica* **2002**, *53*, 175–177.
33. von Quadt, A.; Peytcheva, I.; Cvetkovic, V. Geochronology, geochemistry and isotope tracing of the Cretaceous magmatism of East Serbia and Panagyurishte district (Bulgaria) as part of the Apuseni-Timok-Srednogie metallogenic belt in Eastern Europe. In Proceedings of the 7th Biennial SGA Meeting, Athens, Greece, 24–28 August 2003; Eliopoulos, D.E., Ed.; Society for Geology Applied to Mineral Deposits: Geneva, Switzerland, 2003; pp. 407–410.
34. Drovenik, M.; Antonijević, I.; Mičić, I. New reference on magmatism and geological setting of the Timok Eruptive Area. *Vesn. Geozavoda* **1962**, *20*, 67–79.
35. Živković, P. Petrology and Alterations of Čoka Marin 1 Ore Deposit. Master's Thesis, Faculty of Mining and Geology, Belgrade University, Belgrade, Serbia, 1987. (In Serbian).
36. Pačevski, A.; Moritz, R.; Kouzmanov, K.; Marquardt, K.; Živković, P.; Cvetković, L. Texture and composition of Pb-bearing pyrite from the Čoka Marin polymetallic deposit, Serbia, controlled by nanoscale inclusions. *Can. Mineral.* **2012**, *50*, 1–20. [[CrossRef](#)]
37. Van der Toorn, J.; Davidović, D.; Hadijeva, N.; Strmbanović, I.; Márton, I.; Knaak, M.; Tosdal, R.M.; Davis, B.; Hasson, S. A new sedimentary rock-hosted gold belt in eastern Serbia. In Proceedings of the 12th Biennial SGA Meeting—Mineral deposit research for a high-tech world, Uppsala, Sweden, 12–15 August 2013; Jonsson, E., Ed.; Society for Geology Applied to Mineral Deposits: Geneva, Switzerland, 2013; Volume 2, pp. 691–694.
38. Pačevski, A.; Cvetković, V.; Šarić, K.; Banješević, M.; Hofer, H.E.; Kremenović, A. Manganese mineralization in andesites of Brestovačka Banja, Serbia: Evidence of sea-floor exhalations in the Timok Magmatic Complex. *Mineral. Petrol.* **2016**, *110*, 491–502. [[CrossRef](#)]

39. Paton, C.; Hellstrom, J.; Paul, B.; Woodhead, J.; Hergt, J. Iolite: Freeware for the visualisation and processing of mass spectrometric data. *J. Anal. At. Spectrom.* **2011**, *26*, 2508–2518. [[CrossRef](#)]
40. Jackson, S.; Pearson, N.; Griffin, W.; Belousova, E. The application of laser ablation-inductively coupled plasma-mass spectrometry to in situ U-Pb zircon geochronology. *Chem. Geol.* **2004**, *211*, 47–69. [[CrossRef](#)]
41. Wiedenbeck, M.; Allé, P.; Corfu, F.; Griffin, W.L.; Meier, M.; Oberli, F.; von Quadt, A.; Roddick, J.C.; Spiegel, W. Three natural zircon standards for U-Th-Pb, Lu-Hf, trace element and REE analyses. *Geostand. Newsl.* **1995**, *19*, 1–23. [[CrossRef](#)]
42. Black, L.P.; Kamo, S.L.; Allen, C.M.; Aleinikoff, J.N.; Davis, D.W.; Korsch, R.J.; Foudoulis, C. TEMORA 1: A new zircon standard for Phanerozoic U–Pb geochronology. *Chem. Geol.* **2003**, *200*, 155–170. [[CrossRef](#)]
43. Sláma, J.; Košler, J.; Condon, D.J.; Crowley, J.L.; Gerdes, A.; Hanchar, J.M.; Horstwood, M.S.A.; Morris, G.A.; Nasdala, L.; Norberg, N.; et al. Plešovice zircon—A new natural reference material for U–Pb and Hf isotopic microanalysis. *Chem. Geol.* **2008**, *249*, 1–35. [[CrossRef](#)]
44. von Quadt, A.; Wotzlaw, J.F.; Buret, Y.; Large, S.J.E.; Peytcheva, I.; Trinquier, A. High-precision zircon U/Pb geochronology by ID-TIMS using new 10^{13} ohm resistors. *J. Anal. At. Spectrom.* **2016**, *31*, 658–665. [[CrossRef](#)]
45. Petrus, J.A.; Kamber, B.S. Vizual Age: A Novel Approach to Laser Ablation ICP-MS U-Pb Geochronology Data Reduction. *Geostand. Geoanal. Res.* **2012**, *36/3*, 247–270. [[CrossRef](#)]
46. Vermeesch, P. IsoplotR: A free and open toolbox for geochronology. *Geosci. Front.* **2018**, *9*, 1479–1493. [[CrossRef](#)]
47. Ljubović-Obradović, D.; Carevac, I.; Mirković, M.; Protić, N. Upper Cretaceous volcanoclastic-sedimentary formations in the Timok Eruptive Area (eastern Serbia): New biostratigraphic data from planktonic foraminifera. *Geol. Carpathica* **2011**, *62*, 435–446. [[CrossRef](#)]
48. Banješević, M. Upper Cretaceous magmatic suites of the Timok Magmatic Complex. *Ann. Geol. Penins. Balk.* **2010**, *71*, 13–22. [[CrossRef](#)]
49. Globe Newswire, Press Release Distribution Services. Available online: <https://www.marketwired.com> (accessed on 16 July 2019).
50. Banješević, M. Upper Cretaceous Magmatism of the Timok Magmatic Complex. Ph.D. Thesis, Belgrade University, Belgrade, Serbia, 2006. (In Serbian).
51. Kolb, M. Geochronology and Isotope Geochemistry of Magmatic Rocks from Western Srednogorie (Bulgaria) and Timok Magmatic Complex (East Serbia). Ph.D. Thesis, ETH Zurich, Zurich, Switzerland, 2011.
52. Defant, M.J.; Drummond, M.S. Derivation of some modern arc magmas by melting of young subducted lithosphere. *Nature* **1990**, *347*, 662–665. [[CrossRef](#)]
53. Castillo, P.R. Adakite petrogenesis. *Lithos* **2006**, *134–135*, 304–316. [[CrossRef](#)]
54. Oyarzun, R.; Marquez, A.; Lillo, J.; Lopez, I.; Rivera, S. Giant versus small porphyry copper deposits of Cenozoic age in Northern Chile: Adakite versus normal calc-alkaline magmatism. *Miner. Depos.* **2001**, *36*, 794–798. [[CrossRef](#)]
55. Richards, J.P.; Kerrich, R. Adakite-like rocks: Their diverse origins and questionable role in metallogenesis. *Econ. Geol.* **2007**, *102*, 537–576. [[CrossRef](#)]
56. Bissig, T.; Leal-Mejía, H.; Stevens, R.B.; Hart, C.J.R. High Sr/Y Magma Petrogenesis and the Link to Porphyry Mineralization as Revealed by Garnet-Bearing I-Type Granodiorite Porphyries of the Middle Cauca Au-Cu Belt, Colombia. *Econ. Geol.* **2017**, *112*, 551–568. [[CrossRef](#)]
57. Chiaradia, M. Adakite-like magmas from fractional crystallization and melting-assimilation of mafic lower crust (Eocene Macuchi arc, Western Cordillera, Ecuador). *Chem. Geol.* **2009**, *265*, 468–487. [[CrossRef](#)]
58. Chung, S.L.; Liu, D.Y.; Ji, J.Q.; Chu, M.F.; Lee, H.Y.; Wen, D.J.; Lo, C.H.; Lee, T.Y.; Qian, Q.; Zhang, Q. Adakites from continental collision zones: Melting of thickened lower crust beneath southern Tibet. *Geology* **2003**, *31*, 1021–1024. [[CrossRef](#)]
59. Macpherson, C.; Dreher, S.; Thirlwall, M. Adakites without slab melting: High pressure differentiation of island arc magma, Mindanao, the Philippines. *Earth Planet. Sci. Lett.* **2006**, *243*, 581–593. [[CrossRef](#)]
60. Wang, Q.; Xu, J.F.; Jian, P.; Bao, Z.W.; Zhao, Z.H.; Li, C.F.; Xiong, X.L.; Ma, J.L. Petrogenesis of adakitic porphyries in an extensional tectonic setting, Dexing, South China: Implications for the genesis of porphyry copper mineralization. *J. Petrol.* **2006**, *47*, 119–144. [[CrossRef](#)]
61. Audétat, A.; Simon, A.C. Magmatic controls on porphyry copper deposits. *Soc. Econ. Geol. Spec. Publ.* **2012**, *16*, 573–618.

62. Hedenquist, J.W.; Richards, J.P. The influence of geochemical techniques on the development of genetic models for porphyry copper deposits. In *Techniques in Hydrothermal Ore Deposits Geology*; Richards, J.P., Larson, P.B., Eds.; Society of Economic Geologists: Littleton, CO, USA, 1998; Volume 10, pp. 235–256.
63. Sillitoe, R.H. Gold-rich porphyry deposits: Descriptive and genetic models and their role in exploration and discovery. *Rev. Econ. Geol.* **2000**, *13*, 315–345.
64. Richards, J.P. The oxidation state, and sulfur and Cu contents of arc magmas: Implications for metallogeny. *Lithos* **2015**, *233*, 27–45. [[CrossRef](#)]
65. Grove, T.L.; Elkins-Tanton, L.T.; Parman, S.W.; Chatterjee, N.; Muntener, O.; Gaetani, G.A. Fractional crystallization and mantle-melting controls on calc-alkaline differentiation trends. *Contrib. Mineral. Petrol.* **2003**, *145*, 515–533. [[CrossRef](#)]
66. Barclay, J.; Carmichael, I.S.E. A Hornblende Basalt from Western Mexico: Water-saturated Phase Relations Constrain a Pressure-Temperature Window of Eruptibility. *J. Petrol.* **2004**, *45/3*, 485–506. [[CrossRef](#)]
67. Feig, S.; Koepke, J.; Snow, J.E. Effect of water on tholeiitic basalt phase equilibria: An experimental study under oxidizing conditions. *Contrib. Mineral. Petrol.* **2006**, *152*, 611–638. [[CrossRef](#)]
68. Larocque, J.; Canil, D. The role of amphibole in the evolution of arc magmas and crust: The case from the Jurassic Bonanza arc section, Vancouver Island, Canada. *Contrib. Mineral. Petrol.* **2009**, *159/4*, 475–492. [[CrossRef](#)]
69. Sisson, T.W.; Grove, T.L. Experimental investigations of the role of H₂O in calc-alkaline differentiation and subduction zone magmatism. *Contrib. Mineral. Petrol.* **1993**, *113*, 143–166. [[CrossRef](#)]
70. Alonso-Perez, R.; Muntener, O.; Ulmer, P. Igneous garnet and amphibole fractionation in the roots of island arcs: Experimental constraints on andesitic liquids. *Contrib. Mineral. Petrol.* **2009**, *157*, 542–558. [[CrossRef](#)]
71. Maksimov, A.P. The influence of water on the temperature of amphibole stability in melts. *J. Volcanol. Seismol.* **2009**, *3*, 27–33. [[CrossRef](#)]
72. Burnham, C.W. Magmas and hydrothermal fluids. In *Geochemistry of Hydrothermal Ore Deposits*, 2nd ed.; Barnes, H.L., Ed.; John Wiley and Sons: New York, NY, USA, 1979; pp. 71–136.
73. Candela, P.A. Magmatic ore-forming fluids: Thermodynamic and mass transfer calculations of metal concentrations. In *Ore Deposition Associated with Magmas*; Whitney, J.A., Naldrett, A.J., Eds.; Society of Economic Geologists: El Paso, TX, USA, 1989; Volume 4, pp. 203–221.
74. Hedenquist, J.W.; Lowenstern, J.B. The role of magmas in the formation of hydrothermal ore deposits. *Nature* **1994**, *370*, 519–527. [[CrossRef](#)]
75. Loucks, R.R. Distinctive composition of copper-ore-forming arc magmas. *Aust. J. Earth Sci.* **2014**, *61*, 5–16. [[CrossRef](#)]



© 2019 by the authors. Licensee MDPI, Basel, Switzerland. This article is an open access article distributed under the terms and conditions of the Creative Commons Attribution (CC BY) license (<http://creativecommons.org/licenses/by/4.0/>).